



HAL
open science

An Insight into the photoinduced phenomena in ternary Ge-Sb-Se sputtered thin films

T. Halenkovič, M. Kotrla, J. Gutwirth, V. Nazabal, P. Nemeč

► **To cite this version:**

T. Halenkovič, M. Kotrla, J. Gutwirth, V. Nazabal, P. Nemeč. An Insight into the photoinduced phenomena in ternary Ge-Sb-Se sputtered thin films. *Photonics research*, 2022, 10 (9), pp.2261-2266. 10.1364/PRJ.460552 . hal-03798863

HAL Id: hal-03798863

<https://hal.science/hal-03798863>

Submitted on 23 Nov 2022

HAL is a multi-disciplinary open access archive for the deposit and dissemination of scientific research documents, whether they are published or not. The documents may come from teaching and research institutions in France or abroad, or from public or private research centers.

L'archive ouverte pluridisciplinaire **HAL**, est destinée au dépôt et à la diffusion de documents scientifiques de niveau recherche, publiés ou non, émanant des établissements d'enseignement et de recherche français ou étrangers, des laboratoires publics ou privés.

An insight into the photoinduced phenomena in ternary Ge-Sb-Se sputtered thin films

TOMÁŠ HALENKOVIČ,^{1,*} MAGDALÉNA KOTRLA,¹ JAN GUTWIRTH,¹ VIRGINIE NAZABAL^{2,1} AND PETR NĚMEC^{1,*}

¹Department of Graphic Arts and Photophysics, University of Pardubice, Pardubice, Czech Republic

²Univ Rennes, CNRS, ISCR (Institut des Sciences Chimiques de Rennes) – UMR 6226, F-35000 Rennes, France

*tomas.halenkovic@upce.cz

*petr.nemec@upce.cz

Abstract: The kinetics of photoinduced changes, namely photobleaching and photodarkening in sputtered ternary Ge₂₉Sb₈Se₆₃ thin films was studied. Study of time evolution of absorption coefficient $\Delta\alpha(t)$ upon room-temperature near-bandgap irradiation revealed several types of photoinduced effects. The as-deposited films exhibited a fast photodarkening followed by dominative photobleaching process. Annealed thin films were found to undergo photodarkening only. Local structure studied by Raman scattering spectroscopy showed significant structural changes upon thermal annealing which are presumably responsible for a transition from the photobleaching observed in as-deposited and reversible photodarkening in annealed thin films. Moreover, transient photodarkening process was observed in both as-deposited as well as in annealed thin films. An influence of the initial film thickness and laser optical intensity onto the kinetics of photoinduced changes is discussed.

© 2021 Optica Publishing Group under the terms of the [Optica Publishing Group Open Access Publishing Agreement](#)

1. Introduction

Photostructural changes in amorphous chalcogenide thin films and chalcogenide glasses have been extensively studied for many decades [1]. Chemical bond rearrangement induced by the light excitation having the energy near the bandgap of these materials leads to the modifications of amorphous matrix resulting in changes of optical properties [2]. These are referred to a photodarkening (PD) and a photobleaching (PB) depending on a sign of a change [3]. The magnitude of PD and PB is related to the composition and the structure of chalcogenide materials. While in the binary arsenic-based chalcogenides only PD occurs, both germanium-based binaries [4, 5] and ternaries show rather complex behavior with a sign of the change being a product of a competitive processes of PD and PB [6, 7].

The PD of exposed annealed films of As₂S₃ and As₂Se₃ which may be partially recovered by the consequent annealing was reported as early as in 1970s by De Neufville *et al.* [1]. It is considered that the as-deposited amorphous chalcogenide thin films possess the irreversible photoinduced changes while the annealed films and melt-quenched glasses undergo the reversible ones [8]. Recently, the waveguide inscription using femtosecond lasers (ultrafast laser inscription, ULI) attracted the attention of some researchers [9, 10]. This process includes the nonlinear absorption of sub-bandgap light resulting in changes in refractive index. Results on ULI in Ge-Sb-S glasses by means of structural study suggest that the driving forces of PD during the ULI in chalcogenide glasses are of the same origin as the photostructural changes due to the near-bandgap continuous-wave laser irradiation [10]. A better comprehension of the processes and variables involved in photoinduced phenomena may play an important role for potential applications, optimization and tailoring properties of these materials in field of photonic integrated circuits, holographic gratings and waveguide inscription [11].

47 The aim of this paper is to provide a study of photoinduced changes in Ge-Sb-Se
48 chalcogenide thin films which are of particular interest in the field of photonic integrated
49 circuits for their potential application in non-linear optics [12] and optical sensors in mid-
50 infrared domain [13, 14]. The nominal composition of $\text{Ge}_{25}\text{Sb}_{10}\text{Se}_{65}$ was chosen based on our
51 previous work related to photosensitivity study on this system [15]. It combines favorable
52 optical properties and expected photosensitivity. Relatively high optical bandgap energy causes
53 the orange color of thin films within range of thicknesses under study which in combination
54 with low surface reflectivity allows an easy detection of photoinduced changes. The insight in
55 the photoinduced changes provided in this paper summarizes up to date available references
56 and tries to recognize the challenges in understanding the general principles of these
57 phenomena. The influence of a thickness and the laser optical intensity onto the kinetics of
58 these processes is discussed.
59

60 2. Methods

61 A sputtering target ($\phi = 50$ mm) of $\text{Ge}_{25}\text{Sb}_{10}\text{Se}_{65}$ chalcogenide glass was synthesized by
62 melt-quenching technique described elsewhere [16]. Thin films with thicknesses d of 350, 500,
63 and 650 nm were deposited by rf-sputtering (13.56 MHz) at 5×10^{-3} mbar working pressure of
64 argon onto well-cleaned microscope slides (soda-lime float glass, substrate length of 76 mm).
65 The variance in the thickness was estimated to be $< 6\%$ within the substrate length. Selected
66 thicknesses were found to be optimal for our experiments as the penetration depth of a pump
67 laser described below is ~ 700 and ~ 1800 nm for as-deposited and annealed films, respectively.

68 Composition of thin films was verified by energy-dispersive X-ray spectroscopy (EDS)
69 joint with scanning electron microscope (JEOL IT-300, JEOL Ltd., Japan). X-ray diffraction
70 (XRD) patterns were collected within the range of 2θ from 10° to 80° with a step of 0.02° (Cu
71 K- α , Rigaku, Japan). Thickness of thin films and its initial optical properties, specifically
72 refractive index n and the optical bandgap energy E_g , were determined from variable angle
73 spectroscopic ellipsometry (VASE, J. A. Woollam, USA).

74 Annealing of samples was performed at temperature of 250°C (*i.e.* glass transition
75 temperature of bulk $T_g - 50^\circ\text{C}$) for 2 hours (heating rate of $2^\circ\text{C} \cdot \text{min}^{-1}$, cooling rate of $1^\circ\text{C} \cdot$
76 min^{-1}) under argon atmosphere.

77 Kinetics of photoinduced changes of both as-deposited and annealed samples at the room
78 temperature was studied by means of *in situ* transmittance measurements captured by
79 fiber-coupled high-resolution spectrometer (OceanInsight, USA). Samples were placed in
80 a hermetically sealed cell equipped with quartz windows filled with pure argon gas and
81 irradiated by near-bandgap light coming from 589 nm (2.1 eV) continuous-wave DPSS laser
82 source (Shanghai Laser & Optics Century co., Ltd., China) for 180 minutes. The experimental
83 setup for *in situ* kinetics measurements is depicted in Fig. 1(a). In order to retain the athermal
84 nature of photoinduced changes low to moderate laser optical intensities, specifically 3.0 ± 0.5 ,
85 19.0 ± 2.5 , 50.0 ± 3.0 and 125 ± 5.0 $\text{mW} \cdot \text{cm}^{-2}$ were used.

86 The changes were expressed as the time evolution of absorption coefficient $\Delta\alpha(t)$ calculated
87 as $\Delta\alpha(t) = \ln[T_0 \cdot T(t)^{-1}] \cdot d^{-1}$, where T_0 is the initial transmittance, $T(t)$ is the transmittance at
88 elapsed time t . Selected value of the initial transmittance at irradiation wavelength was $\approx 18\%$,
89 corresponding to the region of exponential absorption edge (Urbach edge, at initial value of
90 absorption coefficient α in order of $\sim 10^4$ cm^{-1}). It is worth to note that the small changes in the
91 thickness are expected during the irradiation (such as photoinduced volume change in As_2S_3
92 chalcogenide glass [17]); however, this effect does not affect the value of $\Delta\alpha$ significantly.
93 Changes in the reflectance during the irradiation were also neglected.

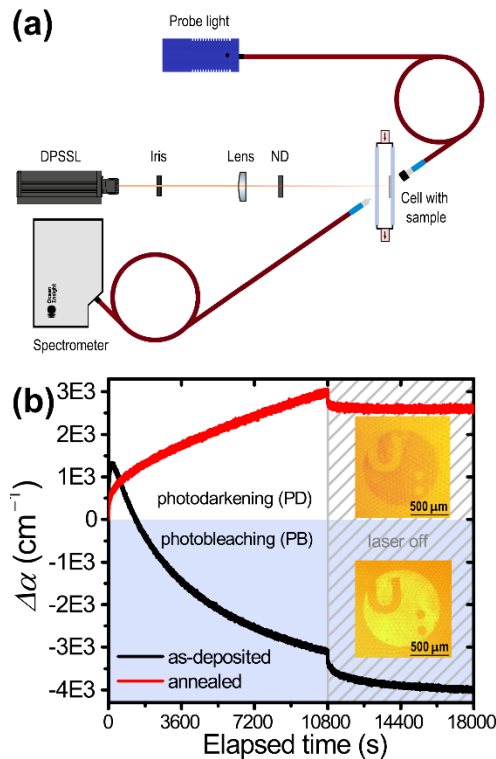
94 The magnitude of absorption edge shift by means of a change of E_g succeeding the
95 irradiation was determined directly from transmittance measurements using WVASE32
96 software (J. A. Woollam, USA). It should be emphasized that the evaluation of absolute values
97 of E_g and its changes was not the target of this work and so the precision of the estimation using
98 this approach is rather coarse with expected accuracy about ± 0.02 eV.

100 **3. Results and Discussion**101 **3.1. Optical properties of thin films**

102 Chemical composition of vitreous target was found to be $\text{Ge}_{24}\text{Sb}_{11}\text{Se}_{66}$ (± 1 at. %). In agreement
 103 with a previous work on this system [16], the slight changes in stoichiometry during the
 104 sputtering process were observed as the composition of thin films was $\text{Ge}_{29}\text{Sb}_8\text{Se}_{63}$ (± 1 at. %).
 105 Optical bandgap energy E_g of as-deposited thin films was 1.87 ± 0.02 eV and the refractive index
 106 n at 1 550 nm is 2.55 ± 0.01 as determined by VASE using Cody-Lorentz oscillator model. An
 107 annealing treatment caused bleaching of thin films resulting in optical bandgap energy increase
 108 to 1.96 ± 0.02 eV accompanied with slight refractive index decrease down to 2.54 ± 0.01 . Both
 109 as-deposited as well as annealed ones were found to be amorphous according the XRD
 110 measurements.

111 As shown in Fig. 1(b) the prolonged irradiation caused the change of an opposite sign,
 112 *i.e.* PB in as-deposited films and PD in annealed ones, reasonably of a highest magnitude when
 113 the laser optical intensity of $125 \text{ mW} \cdot \text{cm}^{-2}$ was used. It should be noted that even after three
 114 hours of irradiation the photoinduced change is not fully saturated and so for the measurements
 115 at lower laser optical intensities the irradiation time was conserved.

116 The highest magnitude of PB by means of an increase in E_g about 0.04 ± 0.02 eV was found
 117 in the sample with the thickness of ~ 350 nm. On the other hand, the highest measure of PD,
 118 specifically the decrease in E_g by 0.05 ± 0.02 eV, was found in sample with thickness of ~ 650
 119 nm at above mentioned conditions.



120

121

122

123

124

Fig. 1. (a) Experimental setup for irradiation setup for *in situ* measurements. A pump beam from DPSSL laser is aimed onto the sample through the plano-convex lens and its desired optical intensity is adjusted by the neutral density filter(s) (ND). (b) A typical time evolution of absorption coefficient $\Delta\alpha(t)$ for as-deposited film (black) and annealed film (red) upon room-

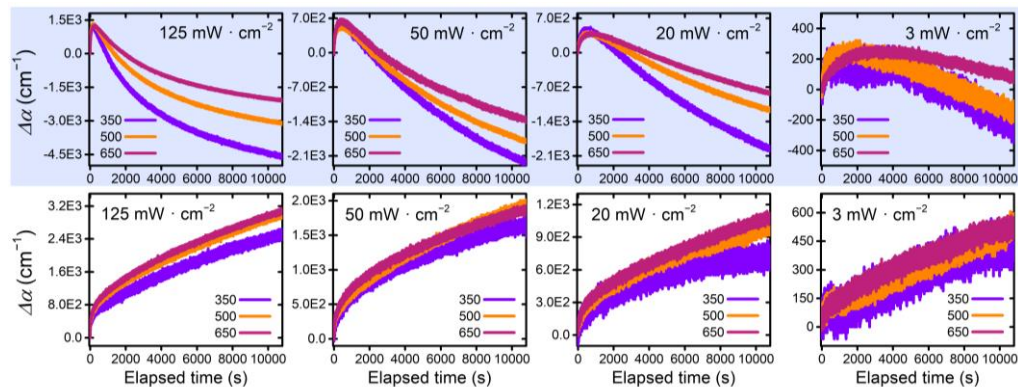
125
126
127
128

temperature irradiation at laser optical intensity of $125 \text{ mW} \cdot \text{cm}^{-2}$; shaded region represents the data acquisition after the laser is switched off; inserts with photodarkened (top) and photobleached (bottom) University of Pardubice logo using 1 mm diameter negative stencil (colors are illustrational only without profiling).

129 3.2 Millisecond kinetics of photoinduced changes

130 Study of time evolution of absorption coefficient $\Delta\alpha(t)$ revealed several types of photoinduced
131 effects. First, as-deposited films exhibit fast PD which is entirely dominated by PB in long-
132 term. Such behavior has already been observed in some as-deposited selenide films *e.g.* in
133 evaporated GeSe_2 [18] and Ge-As-Se [7], pulsed laser deposited Ge-Sb-Se [19] or in
134 cosputtered Ga-Sb-Se [20]. Moreover, only PD takes places during the irradiation of annealed
135 films. Finally, transitory change, specifically transient PD (TPD), was observed in both as-
136 deposited as well as in annealed thin films.

137 As seen in Fig. 2 (top panel), PB in as-deposited thin films is strongly thickness dependent
138 having the magnitude of a process indirectly proportional to the thickness. It is worthy to note
139 that the PB effect in the film with thickness of $\sim 350 \text{ nm}$ (violet curve) is closest to being
140 saturated when irradiated by $125 \text{ mW} \cdot \text{cm}^{-2}$ laser optical intensity. Presumably, the observed
141 PB effect upon prolonged near-bandgap irradiation is of a similar origin as the bleaching upon
142 thermal annealing. Such change is coming from a mutual polymerization of defective entities
143 resulting in ordered structures *via* homo- to heteropolar bond conversion [1]. The excitation
144 generates the charged radiation defects followed by recombination-induced bond
145 rearrangements due to the diffusion of atoms [21]. Although the photoexcited states have not
146 yet been proven experimentally [22], their existence leading to an increased short- and medium-
147 range order [23] is generally accepted explanation of irreversible changes in different properties
148 including absorption edge shift. Other stabilization mechanisms, such as void collapsing [22],
149 evaporation of volatile entities, and the photo-enhanced oxidation [24] may contribute to these
150 changes. As the experiments performed in frame of this work were carried out in a pure argon
151 atmosphere, we do not expect the last mentioned has an important contribution to observed
152 effects.



153
154
155
156
157

Fig. 2. Time evolution of absorption coefficient $\Delta\alpha(t)$ of as-deposited (top panel) and annealed (bottom panel) Ge-Sb-Se thin films upon room-temperature irradiation depending on thicknesses at different laser optical intensities varying from 3 to $125 \text{ mW} \cdot \text{cm}^{-2}$. (This figure should not be reduced).

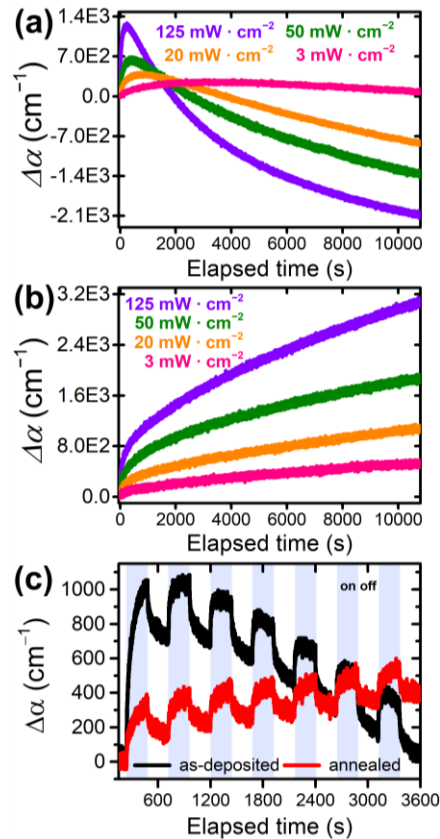
158
159
160
161
162
163

In contrast with PB observed in as-deposited thin films, the PD in annealed thin films as seen in Fig. 2 (bottom panel) is proportionally dependent on the thickness and is a universal process observed in annealed chalcogenide glasses and thin films – *i.e.* reversible photodarkening effect – which may be recovered by thermal annealing. The mechanism of reversible changes is not yet known as no subtle structural changes have yet been experimentally determined. They are likely the result of a similar elemental process as the

164 irreversible ones, *i.e.* recombination-induced bond rearrangements and atom motions [3].
 165 Presumably, the reversible photodarkening is coming from the valence band broadening
 166 resulting in the red-shift [22].

167 The origin of fast PD in as-deposited films is not yet fully understood. Sati and Jain [6]
 168 proposed that it originates in homo- to heteropolar bond conversion at deformed sites such as
 169 Se–Se dimers at the $[\text{GeSe}_{4/2}]$ or Sb–Sb bonds caused by Sb–Sb–Se in defective $[\text{SbSe}_{3/2}]$
 170 pyramidal units, present in evaporated Ge-Sb-Se thin films, and is simply a competitive process
 171 to slow PB which becomes dominant in long-term. Relative to time, the magnitude of PB is
 172 rather small compared to PD.

173 Besides being thickness dependent, fast PD and slow PB in as-deposited and reversible PD
 174 in annealed Ge-Sb-Se thin films are strongly dependent on laser optical intensity as depicted in
 175 Fig. 3(a) and (b) respectively. The time evolution of fast PD shows a saturation at $125 \text{ mW} \cdot \text{cm}^{-2}$
 176 within $\sim 245 \text{ s}$ and clearly delays with a decreasing intensity. Similar observation
 177 was reported for evaporated Ge-As-Se films by Khan *et al.* [25]. The process of fast PD
 178 becomes completely dominated by slow PB process.



179

180

181

182

183

184

Fig. 3. (a) Time evolution of absorption coefficient $\Delta\alpha(t)$ of as-deposited and (b) annealed Ge-Sb-Se thin films with thickness of $\sim 650 \text{ nm}$ depending on the laser optical intensity. (c) On/off cycles (240 s) experiment with as-deposited (black line) and annealed (red line) Ge-Sb-Se thin films with the same thickness using laser optical intensity of $50 \text{ mW} \cdot \text{cm}^{-2}$. The shaded area corresponds to the cycle when the laser is switched on.

185

186

187

188

Transitory changes by means of transient PD (TPD) were easily noticed by on/off experiments found in Fig. 3(c). TPD has already been observed by various authors [7, 19, 26-29] and may be related to a phenomenon termed as an ‘optical stopping effect’ by Matsuda *et al.* back in 1970s [30]. Ganjoo *et al.* [27] observed TPD in annealed evaporated amorphous

189 selenium a-Se and As_2Se_3 of ~ 500 nm thickness when irradiated by Ar ion laser ($\lambda = 514$ nm,
190 optical intensity of $80 \text{ mW} \cdot \text{cm}^{-2}$). An apparent rise in the transmittance after switching the
191 laser off ($\lambda = 488$ and 660 nm, $150 \text{ mW} \cdot \text{cm}^{-2}$) was also reported for $1 \mu\text{m}$ thick as-deposited
192 GeSe_2 and Ge_2Se_3 evaporated films by Yan *et al.* [28]. Similar behavior was found in sputtered
193 as-deposited Ge-As-Se thin films at different intensities when exposed to 655 nm laser diode
194 [29]. Additionally, the magnitude of TPD among the references herein seems to be affected by
195 the optical intensity and the metastable PD or PD depending on composition. The structural
196 origin of TPD is yet to be understood. *In situ* EXAFS experiments on amorphous selenium
197 indicate that it may be associated to a chalcogen coordination number increase upon irradiation
198 [22, 31].

199 Finally, the results on millisecond kinetics of photoinduced changes in as-deposited
200 and annealed Ge-Sb-Se thin films suggest that they are of a very same origin as in Ge-As-Se
201 system [29]. Even though the sign and the magnitude of a change may differ with a composition
202 and the structure [5, 7, 15], the TPD and reversible PD in annealed thin films seem to be a
203 universal feature of photoinduced changes in amorphous chalcogenides.
204

205 3.3 Structural changes upon annealing and the irradiation

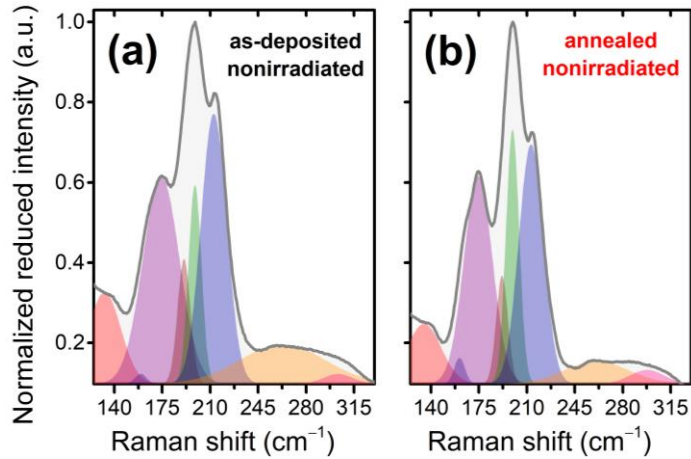
206 Changes in local structure upon thermal annealing and irradiation were investigated using
207 Raman scattering spectroscopy measurements. As depicted in Fig. 4, the Raman spectra of Ge-
208 Sb-Se thin films are *prima facie* dominated by the band peaking at $\sim 199 \text{ cm}^{-1}$, which
209 corresponds to A_1 symmetric stretching vibrations of heteropolar Ge-Se bonds in a corner-
210 sharing $[\text{GeSe}_{4/2}]$ tetrahedra. The companion mode A_1^c assigned to edge-sharing tetrahedral
211 units is located at $\sim 214 \text{ cm}^{-1}$, [32]. Overlapping E_1 mode of $[\text{SbSe}_{3/2}]$ pyramidal units around
212 $\sim 191 \text{ cm}^{-1}$ may contribute to the Raman intensity of A_1 mode [33]. Peak around $\sim 174 \text{ cm}^{-1}$ is
213 considered to be coming from Ge-Ge homopolar bonds in ethane-like $[\text{Ge}_2\text{Se}_{6/2}]$ units [34].
214 Vibrational modes of Sb-Sb in $[\text{Se}_2\text{Sb-SbSe}_2]$ found at $\sim 160 \text{ cm}^{-1}$ probably contribute to this
215 peak [35].

216 In order to justify changes in the structure, Raman spectra were deconvoluted using 8
217 Gaussian peaks. Besides five peaks mentioned above, the rotational modes in selenium
218 polymeric chains ($\sim 140 \text{ cm}^{-1}$, [35]) and bending vibrational modes of Se-Se at the outrigger
219 ($135\text{--}145 \text{ cm}^{-1}$, [36]) are altogether represented by Gaussian peak centered at $\sim 134 \text{ cm}^{-1}$. A_1
220 vibrational mode of Se_n chains in amorphous selenium found at $\sim 235 \text{ cm}^{-1}$, stretching
221 vibrational modes of Se-Se bonds at the outrigger ($\sim 245 \text{ cm}^{-1}$), A_1 vibrational modes of Se-Se
222 dimers and short Se_n chains in corner-linked $[\text{GeSe}_{4/2}]$, ($\sim 260\text{--}265 \text{ cm}^{-1}$, [35]), and Ge-Ge
223 homopolar bonds' vibrations coming from $[\text{Ge-Ge}_m\text{Se}_{4-m}]$ ($m = 1, 2, 3, 4$), found $\sim 270 \text{ cm}^{-1}$
224 [34] are collectively represented by Gaussian at $\sim 262 \text{ cm}^{-1}$. Finally, F_1 asymmetric vibrational
225 modes of GeSe_4 tetrahedrons are found at $\sim 300 \text{ cm}^{-1}$, [32].

226 Upon thermal annealing an apparent change in the ratio between A_1 (green) and A_1^c (blue)
227 peaks occurred. Simultaneous decrease in the intensity of a peak centered at $\sim 134 \text{ cm}^{-1}$ (red)
228 and $\sim 262 \text{ cm}^{-1}$ (orange) indicates the consumption of selenium atoms as a consequence of
229 increased local order. Other noticeable changes occurred around $\sim 174 \text{ cm}^{-1}$ peak. These
230 changes may be due to a decrease of Ge-Ge homopolar bonds in ethane-like $[\text{Ge}_2\text{Se}_{6/2}]$ units.
231 Changes in intensity of surrounding peaks upon thermal annealing are low and difficult
232 to justify.

233 Photostructural changes by means of Raman scattering spectroscopy have already been
234 described by several authors. The bond breaking mechanism upon the irradiation followed by
235 bond rearrangement and/or crystallization of structural sites are usually connected with changes
236 in optical properties (*i.e.* shift of the absorption edge and the refractive index changes upon
237 irradiation) [4, 7, 37]. Noteworthy, even in highly photosensitive composition of As_2S_3 , the
238 fully saturated PD process results in only up to 1 % of nearest neighbors bonds' alteration at
239 available atomic sites [2]. As only low to moderate laser optical intensities were used in the

240 present study negligible changes in Raman spectra were observed and do not allow a fine
241 analysis of the mechanisms involved.
242



243
244 Fig. 4. (a) Normalized reduced intensity of Raman spectra of nonirradiated as-deposited, and
245 (b) nonirradiated annealed Ge-Sb-S thin films.

246 It can be assumed that above mentioned structural changes upon thermal annealing are
247 responsible for a transition from the PB observed in as-deposited and reversible PD in annealed
248 Ge-Sb-Se thin films respectively. In addition, although the experiments were carried out under
249 the pure argon atmosphere the photo-enhanced oxidation should be not completely ruled out
250 from the contribution to the photoinduced changes as the concentration of germanium is ~ 29
251 at. % [38].

252 4. Conclusions

253 Comprehensive study of photosensitivity in amorphous $\text{Ge}_{29}\text{Sb}_8\text{Se}_{63}$ thin films by means of
254 time evolution of the absorption coefficient $\Delta\alpha(t)$ revealed several types of photoinduced effects
255 in these materials. Fast PD followed by slow dominative PB process is present in
256 as-deposited films while only PD takes places during prolonged irradiation of annealed films.
257 The structural changes upon thermal annealing seem to be responsible for a transition from the
258 PB observed in as-deposited and reversible PD in annealed thin films. Transient PD (TPD) was
259 observed in both as-deposited as well as in annealed thin films and, together with a PD in
260 annealed films, seems to be a universal feature of photoinduced changes in amorphous
261 chalcogenides. The processes behind metastable PD and PB in the as-deposited films as well
262 as TPD, which seem to be associated with transitory photoexcited states, remain to be better
263 understood. Furthermore, the throughout study of surface and thickness changes upon the
264 irradiation and annealing as well as long-term stability at normal room conditions in similar
265 systems are also of interest. Such investigations may lead towards the implementation of these
266 materials and photonic processes in them in the design and engineering of photonic integrated
267 circuits by means of tailoring and optimization of optical properties and inscription of tree-
268 dimensional structures (*e.g.* waveguides, holographic gratings and diffractive optics elements).

269 Funding

270 Czech Science Foundation (project No. 22-05179S). Ministry of Education, Youth and Sports
271 of the Czech Republic (project No. LM2018103).

272

273 Disclosures

274 The authors declare that they have no competing financial interests.

275

276 Data availability

277 Data underlying the results presented in this paper are not publicly available at this time but
278 may be obtained from the authors upon reasonable request.

279

280

281 References

- 282 1. J. P. De Neufville, S. C. Moss, and S. R. Ovshinsky, "Photostructural transformations in amorphous As₂Se₃
283 and As₂S₃ films," *Journal of Non-Crystalline Solids* **13**, 191-223 (1974).
- 284 2. S. Ducharme, J. Hautala, and P. C. Taylor, "Photodarkening profiles and kinetics in chalcogenide glasses,"
285 *Physical Review B* **41**, 12250-12259 (1990).
- 286 3. H. Fritzsche, "The origin of reversible and irreversible photostructural changes in chalcogenide glasses,"
287 *Philosophical Magazine Part B* **68**, 561-572 (1993).
- 288 4. R. R. Kumar, A. R. Barik, E. M. Vinod, M. Bapna, K. S. Sangunni, and K. V. Adarsh, "Crossover from
289 photodarkening to photobleaching in a-GeSe_{100-x} thin films," *Opt. Lett.* **38**, 1682-1684 (2013).
- 290 5. T. Halenkovič, J. Gutwirth, T. Kuriakose, M. Bouška, M. Chauvet, G. Renversez, P. Němec, and V. Nazabal,
291 "Linear and nonlinear optical properties of co-sputtered Ge-Sb-Se amorphous thin films," *Opt. Lett.* **45**, 1523-
292 1526 (2020).
- 293 6. D. C. Sati and H. Jain, "Coexistence of photodarkening and photobleaching in Ge-Sb-Se thin films," *Journal of*
294 *Non-Crystalline Solids* **478**, 23-28 (2017).
- 295 7. P. Khan, H. Jain, and K. V. Adarsh, "Role of Ge:As ratio in controlling the light-induced response of a-
296 GeAs_{35-x}Se₆₅ thin films," *Scientific Reports* **4**, 4029 (2014).
- 297 8. G. Pfeiffer, M. A. Paesler, and S. C. Agarwal, "Reversible photodarkening of amorphous arsenic chalcogens,"
298 *Journal of Non-Crystalline Solids* **130**, 111-143 (1991).
- 299 9. A. Arriola, S. Gross, M. Ams, T. Gretzinger, D. Le Coq, R. P. Wang, H. Ebendorff-Heidepriem, J. Sanghera, S.
300 Bayya, L. B. Shaw, M. Ireland, P. Tuthill, and M. J. Withford, "Mid-infrared astrophotonics: study of ultrafast
301 laser induced index change in compatible materials," *Opt. Mater. Express* **7**, 698-711 (2017).
- 302 10. G. Torun, A. Yadav, K. A. Richardson, and Y. Bellouard, "Ultrafast Laser Direct-Writing of Self-Organized
303 Microstructures in Ge-Sb-S Chalcogenide Glass," *Frontiers in Physics* **10**(2022).
- 304 11. A. Zakery and S. R. Elliott, "Optical properties and applications of chalcogenide glasses: a review," *Journal of*
305 *Non-Crystalline Solids* **330**, 1-12 (2003).
- 306 12. E. Delcourt, N. Jebali, L. Bodiou, M. Baillieul, E. Baudet, J. Lemaitre, V. Nazabal, Y. Dumeige, and J.
307 Charrier, "Self-phase modulation and four-wave mixing in a chalcogenide ridge waveguide," *Opt. Mater.*
308 *Express* **10**, 1440-1450 (2020).
- 309 13. M. Baillieul, E. Baudet, K. Michel, J. Moreau, P. Němec, K. Boukerma, F. Colas, J. Charrier, B. Bureau, E.
310 Rinnert, and V. Nazabal, "Toward Chalcogenide Platform Infrared Sensor Dedicated to the In Situ Detection of
311 Aromatic Hydrocarbons in Natural Waters via an Attenuated Total Reflection Spectroscopy Study," *Sensors* **21**,
312 2449 (2021).
- 313 14. V. Mittal, G. Z. Mashanovich, and J. S. Wilkinson, "Perspective on Thin Film Waveguides for on-Chip Mid-
314 Infrared Spectroscopy of Liquid Biochemical Analytes," *Analytical Chemistry* **92**, 10891-10901 (2020).
- 315 15. T. Halenkovič, J. Gutwirth, P. Němec, E. Baudet, M. Specht, Y. Gueguen, J.-C. Sangleboeuf, and V. Nazabal,
316 "Amorphous Ge-Sb-Se thin films fabricated by co-sputtering: Properties and photosensitivity," *Journal of the*
317 *American Ceramic Society* **101**, 2877-2887 (2018).
- 318 16. F. Verger, V. Nazabal, F. Colas, P. Němec, C. Cardinaud, E. Baudet, R. Chahal, E. Rinnert, K. Boukerma, I.
319 Peron, S. Deputier, M. Guilloux-Viry, J. P. Guin, H. Lhermite, A. Moreac, C. Compère, and B. Bureau, "RF
320 sputtered amorphous chalcogenide thin films for surface enhanced infrared absorption spectroscopy," *Opt.*
321 *Mater. Express* **3**, 2112-2131 (2013).
- 322 17. K. Tanaka, "Photoexpansion in As₂S₃ glass," *Physical Review B* **57**, 5163-5167 (1998).
- 323 18. A. R. Barik, R. Naik, and K. V. Adarsh, "Unusual observation of fast photodarkening and slow photobleaching
324 in a-GeSe₂ thin film," *Journal of Non-Crystalline Solids* **377**, 179-181 (2013).
- 325 19. M. Olivier, R. Boidin, P. Hawlová, P. Němec, and V. Nazabal, "Kinetics of photosensitivity in Ge-Sb-Se thin
326 films," in *2015 International Conference on Photonics, Optics and Laser Technology (PHOTOPTICS)*, 2015,
327 61-66.
- 328 20. T. Halenkovič, J. Gutwirth, M. Bouška, L. Calvez, P. Němec, and V. Nazabal, "Amorphous Ga-Sb-Se thin
329 films fabricated by co-sputtering," *Opt. Lett.* **45**, 29-32 (2020).
- 330 21. Y. S. Kaganovskii, H. Genish, and M. Rosenbluh, "Laser Recording in Chalcogenide Glass Films: Driving
331 Forces and Kinetics of the Mass Transfer," *physica status solidi (a)* **217**, 2000523 (2020).
- 332 22. K. Tanaka and K. Shimakawa, "Light-Induced Phenomena," in *Amorphous Chalcogenide Semiconductors and*
333 *Related Materials* (Springer International Publishing, Cham, 2021), pp. 163-226.

- 334
335
336
337
338
339
340
341
342
343
344
345
346
347
348
349
350
351
352
353
354
355
356
357
358
359
360
361
362
363
364
365
366
367
368
23. L. Tichý, V. Smrčka, H. Tichá, E. Sleetcx, and P. Nagels, "On the origin of photo-induced and thermally induced irreversible bleaching of amorphous Ge-Se films," *Philosophical Magazine Letters* **68**, 73-79 (1993).
 24. C. A. Spence and S. R. Elliott, "Light-induced oxidation and band-edge shifts in thermally evaporated films of germanium chalcogenide glasses," *Physical Review B* **39**, 5452-5463 (1989).
 25. P. Khan, A. R. Barik, E. M. Vinod, K. S. Sangunni, H. Jain, and K. V. Adarsh, "Coexistence of fast photodarkening and slow photobleaching in Ge₁₉As₂₁Se₆₀ thin films," *Opt. Express* **20**, 12416-12421 (2012).
 26. K. Shimakawa and Y. Ikeda, "Transient responses of photodarkening and photoinduced volume change in amorphous chalcogenide films," *Journal of Optoelectronics and Advanced materials* **8**(2006).
 27. A. Ganjoo, K. Shimakawa, K. Kitano, and E. A. Davis, "Transient photodarkening in amorphous chalcogenides," *Journal of Non-Crystalline Solids* **299-302**, 917-923 (2002).
 28. Q. Yan, H. Jain, J. Ren, D. Zhao, and G. Chen, "Effect of Photo-Oxidation on Photobleaching of GeSe₂ and Ge₂Se₃ Films," *The Journal of Physical Chemistry C* **115**, 21390-21395 (2011).
 29. Z. Zhang, S. Xu, Y. Chen, X. Shen, and R. Wang, "Photo-induced effects in Ge-As-Se films in various states," *Opt. Mater. Express* **10**, 540-548 (2020).
 30. A. Matsuda, H. Mizuno, T. Takayama, M. Saito, and M. Kikuchi, "Stopping effect" on guided light in As-S films by a laser beam," *Applied Physics Letters* **24**, 314-315 (1974).
 31. A. V. Kolobov, H. Oyanagi, K. Tanaka, and K. Tanaka, "Structural study of amorphous selenium by in situ EXAFS: Observation of photoinduced bond alternation," *Physical Review B* **55**, 726-734 (1997).
 32. P. Němec, B. Frumarová, and M. Frumar, "Structure and properties of the pure and Pr³⁺-doped Ge₂₅Ga₅Se₇₀ and Ge₃₀Ga₅Se₆₅ glasses," *Journal of Non-Crystalline Solids* **270**, 137-146 (2000).
 33. Z. G. Ivanova, E. Cernoskova, V. S. Vassilev, and S. V. Boycheva, "Thermomechanical and structural characterization of GeSe₂-Sb₂Se₃-ZnSe glasses," *Materials Letters* **57**, 1025-1028 (2003).
 34. K. Jackson, A. Briley, S. Grossman, D. V. Porezag, and M. R. Pederson, "Raman-active modes of a-GeSe₂ and a-GeS₂: A first-principles study," *Physical Review B* **60**, R14985-R14989 (1999).
 35. M. Olivier, J. C. Tchahame, P. Němec, M. Chauvet, V. Besse, C. Cassagne, G. Boudebs, G. Renversez, R. Boidin, E. Baudet, and V. Nazabal, "Structure, nonlinear properties, and photosensitivity of (GeSe₂)_{100-x}(Sb₂Se₃)_x glasses," *Opt. Mater. Express* **4**, 525-540 (2014).
 36. E. Baudet, C. Cardinaud, A. Girard, E. Rinnert, K. Michel, B. Bureau, and V. Nazabal, "Structural analysis of RF sputtered Ge-Sb-Se thin films by Raman and X-ray photoelectron spectroscopies," *Journal of Non-Crystalline Solids* **444**, 64-72 (2016).
 37. S. Zhang, Y. Chen, R. Wang, X. Shen, and S. Dai, "Observation of photobleaching in Ge-deficient Ge_{16.8}Se_{83.2} chalcogenide thin film with prolonged irradiation," *Scientific Reports* **7**, 14585 (2017).
 38. L. Tichý, H. Tichá, K. Handlíř, and K. Jurek, "Photoinduced bleaching of Ge₃₅S₆₅ amorphous film," *Journal of Non-Crystalline Solids* **101**, 223-226 (1988).